

Finite-Control-Set Predictive Current Control Based Real and Reactive Power Control of Grid-Connected Hybrid Modular Multilevel Converter

Rashmi Ranjan Behera, Amarnath Thakur

Department of EEE, National Institute of Technology Jamshedpur, India

Article Info

Article history:

Received Oct 14, 2017

Revised Nov 27, 2017

Accepted Feb 07, 2018

Keyword:

Grid Connected System
Modular Multilevel Converter
Predictive Current Control
Real and Reactive Power Control

ABSTRACT

This paper proposes a modified three-phase topology of Modular Multilevel Converter (MMC) and its application in grid connection of distributed dc generations. This topology has reduced number of switch counts compared to the conventional MMC, eliminates the problem of circulating current and having higher efficiency. A single dc source is required to produce sinusoidal outputs. The number of sub-modules (SMs) in this topology is half of the SMs required in case of MMC, in addition to a single H-bridge circuit per phase. This paper presents a finite-control-set predictive current control scheme (FCS-PCC) for the grid connected dc source through the proposed Hybrid Modular Multilevel Converter (HMMC). This controller controls the desired real and reactive power demand of the grid instantaneously. The simulation study of a three phase grid connected system has been done in Matlab/Simulink and the results are provided for the different real and reactive power demands, to validate the concepts.

Copyright © 2018 Institute of Advanced Engineering and Science.
All rights reserved.

Corresponding Author:

Rashmi Ranjan Behera,
National Institute of Technology Jamshedpur
Dept. of EEE, National Institute of Technology Jamshedpur, India
Email: rashmiranjan1011@gmail.com

1. INTRODUCTION

The multilevel voltage source converters are quite popular power electronics solutions to the medium to high-voltage applications. Several multilevel topologies are being commercialized, such as Neutral Point Clamp (NPC), Flying Capacitor (FC) and Cascaded H-bridge (CHB) [1]. These topologies have some technical challenges, like NPC and FC are quite become complex to implement if the desired level of output voltage is increased, so these have less scalability issues. And also as they have single integrated structure, if there will be some faults in the converter switches, then the total converter has to be replaced. So for reliability and ease of operation purpose, the multilevel topologies need to be more scalable and so need to be modular. In some extent the CHB topology solve these problems. But again the multilevel topology need to be less complex [2, 3].

After the inception of Modular Multilevel Converter (MMC) in 2003[4], this topology became a popular alternative for the conventional multilevel converters. It has several advantages like modular design, easier scaling of levels, higher efficiency because of less switching components, and excellent output waveforms with less harmonic distortions. This topology utilizes the submodules (SMs) for the creation of levels. The SMs have several configurations, from where the half bridge-based SM (HBSM) is quite popular for its simplicity in operation. The schematic of the MMC and a HBSM is shown in Figure 1(a) and 1(b) respectively [4]-[10]. The HBSM is composed of two power electronics switches and a capacitor across them. However this topology requires two dc supplies and two arms of SMs for the sinusoidal output waveforms as shown in Figure 1(a). This topology also suffers from the problem of inherent circulating

current between the arms due to the capacitor imbalances, which require a separate control scheme to minimize through capacitor voltage balancing [7].

To address all these issues, modified hybrid MMC topology is proposed in [15], as shown in Figure 1(c). This topology utilizes only one arm of SMs per phase along with a H-bridge circuit across the load for the generation of sinusoidal outputs [15]. As compared to the MMC this HMMC is having half of the SMs with one H-bridge, so less switching components. The comparison of number of switches and SMs with the MMC is given in Table 1. Due to less switch counts this topology is more efficient and having less complex circuitry. This design is having less energy storing components, which makes this more compact and lesser cost. In this paper one of it's application area of grid connected dc sources, suitably for renewable distributed generations (DGs) has been investigated.

The control of grid connected converters is a very much challenging task because of frequent load variations, which needs to support frequent real and reactive power demand by the grid. Therefore the DGs have to provide required real and reactive power to stabilize the grid power. Various control schemes for this purpose have been published based on proportional plus integral (PI) controllers. As this application is Multi Input Multi Output (MIMO) kind of system, therefore multiple PI controllers need to be applied for the desired control action. The problem with these PI controllers is that these have to be properly tuned, otherwise they can adversely affect the system. Hence these kind of systems need a simpler control schemes. Various advanced control theories have been evolving specially for the power electronics (PEs) applications. The model predictive controller which are usually preferred earlier for the chemical industries, are now becoming popular in applications of PEs, because of it's simpler design, and easier implementation because of evolution of faster microprocessors for faster computations [6], [9]-[14].

This paper presents finite control sets (FCS) based predictive current control technique [11]- [14] for the grid connected dc source through HMMC. This technique is used to find the best switching sequence for the switches of HMMC from the finite switching states, through minimizing a cost function derived from error between the reference and measured grid current. In this work, separate predictive controllers are used for individual phases. Then the simulation study is studied for different real and reactive demand from the grid, whose references were provided manually and the results are shown.

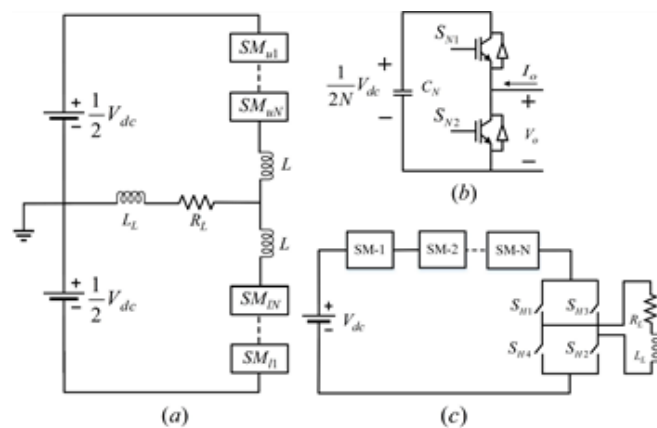


Figure 1. Schematics of (a) Conventional single-phase MMC topology, (b) Half-bridge Sub-Module (SM), (c) Hybrid MMC topology.

2. TOPOLOGY AND BASIC OPERATION

The single-phase topology of HMMC is shown in Figure 1(c). Where a H bridge is connected with an arm of SMs. The three phase grid connected topology is shown in Figure 2. Each SM is composed of a half bridge circuit with two switches and a capacitor across them, as shown in Figure 1(b). On the AC side as shown in Figure 2, the three phases are decoupled through three transformers, T (a, b, c). The HMMC

Table 1. Comparison between conventional MMC and HMMC

	Number of sub-modules	Number of switches	Number of voltage sources
MMC	$2N$	$2 \times 2N$	2
HMMC	$N+1H\text{-Bridge}$	$2N+4$	1

produces output on the AC side as,

$$V_{(a,b,c)} = V \sin(\omega t - x \cdot \frac{2\pi}{3}), \quad x = (0, 1, 2) \quad (1)$$

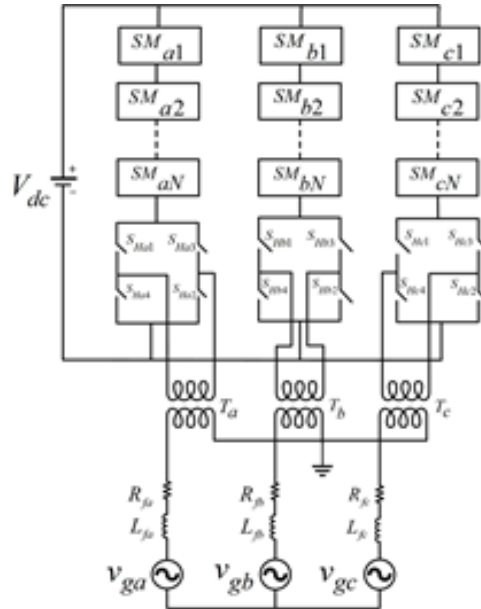


Figure 2. Schematic diagram of three-phase grid-tied HMMC

The SM as shown in Figure 1(b), is said to be connected when the upper switch i.e. S_{n1} in ON and lower switch S_{n2} is OFF, and the SM is bypassed when S_{n1} is OFF and S_{n2} is ON. The switches of the H-bridge are switched at the line frequency i.e. at 50 Hz. The opposite diagonal switch pairs are switched ON and OFF at positive and negative half cycles for the reversal of load current to generate AC at load side.

3. PREDICTIVE CURRENT CONTROL SCHEME

The grid connected three-phase HMMC is controlled by separate predictive current controllers per phase. The primary objective of this controller is to provide the adequate switching sequence to the switches of HMMC to generate desired real and reactive power demand by the grid. The overall system integrated with predictive controller implemented per phase is shown in Figure 3.

The control scheme is divided into three stages, first one is to generate the reference current, formulation of cost function, and then choosing the optimum switching sequence with the minimum error.

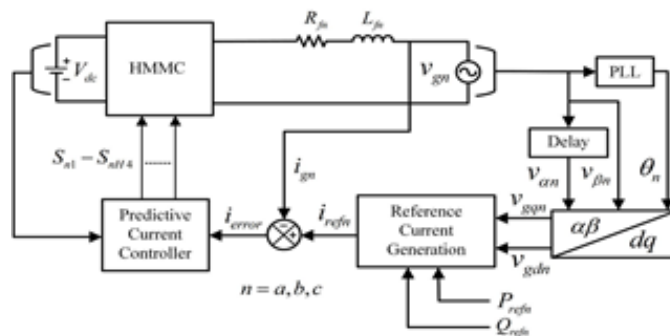


Figure 3. Overall grid connected HMMC system with predictive current control scheme.

3.1. Reference Current Generation

This control scheme is applied for individual phases separately. So the reference current is generated for each phase. In each phase, the first step is to derive the orthogonal signals by sensing the phase current per sample time T_s . Because for the controller, two orthogonal signals from a single signal is necessary to control the real and reactive power separately. Therefore an signal orthogonal to the actual phase voltage is generated. As shown in Figure 4, $v_{\alpha n}$ and $v_{\beta n}$ are the signals orthogonal to each other, where the first one is the actual voltage per phase and the second one is phase shifted by $\pi/2$. The notation n is used for the different phases a, b, c . Now these signal which are in stationary reference frame, converted into the synchronous ($d-q$) reference frame using following equations [11].

$$\begin{bmatrix} v_{gdn} \\ v_{gqn} \end{bmatrix} = \begin{bmatrix} \sin\omega t & -\cos\omega t \\ \cos\omega t & \sin\omega t \end{bmatrix} \begin{bmatrix} v_{g\alpha n} \\ v_{g\beta n} \end{bmatrix} \quad (2)$$

Now from these voltage signals in $d-q$ reference frame and utilizing the reference real and reactive power, the reference current signals in $d-q$ reference frame are calculated using,

$$\begin{bmatrix} i_{drefn} \\ i_{qrefn} \end{bmatrix} = \frac{2}{(v_{gdn}^2) + v_{gqn}^2} \begin{bmatrix} v_{gdn} & v_{gqn} \\ v_{gqn} & -v_{gdn} \end{bmatrix} \begin{bmatrix} P_{refn} \\ Q_{refn} \end{bmatrix} \quad (3)$$

Then the desired reference current to match up with the real and reactive power demand by the grid, is generated by,

$$i_{refn} = \begin{bmatrix} i_{drefn} & i_{qrefn} \end{bmatrix} \begin{bmatrix} \sin\omega t \\ -\cos\omega t \end{bmatrix} \quad (4)$$

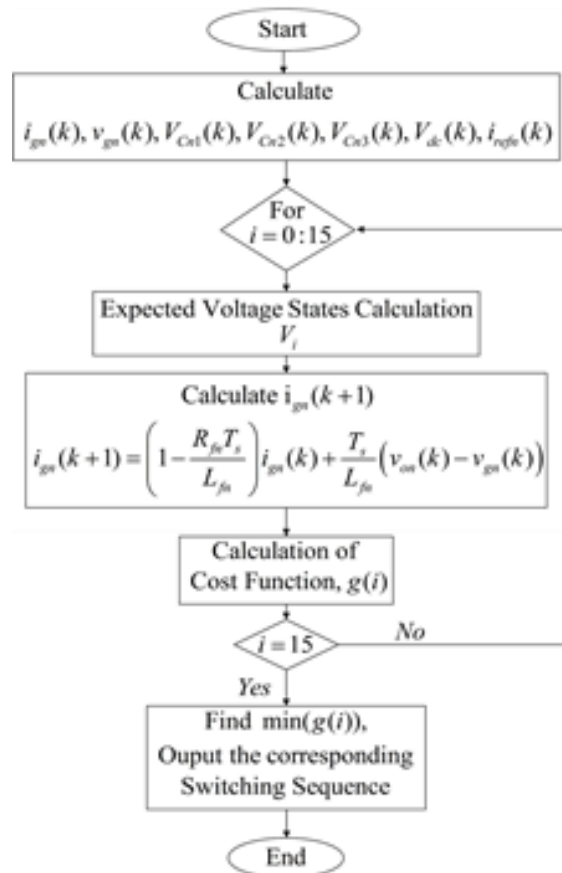


Figure 4. Flowchart of predictive current control algorithm

3.2. Formulation of Cost Function

In this stage, the grid parameters are obtained in a discrete sample time T_s . The actual grid current is discretized, which will further used for the future prediction from the measured grid current and voltage values at sample time k , using the forward-Euler approximation as:

$$\frac{di_{gn}}{dt} = \frac{1}{T_s}(i_{gn}(k+1) - i_{gn}(k)) \quad (5)$$

The future grid current prediction is done by calculating the grid current for each possible voltage states. These voltage states are calculated from the different switching combinations, as shown in Table 2.

Table 2. Switching sequences for different voltage states

Switches	S_{11}	S_{12}	S_{21}	S_{22}	S_{31}	S_{32}	S_{33}	S_{41}	S_{42}	S_{43}
Voltage States										
$+V_{dc}$	0	1	0	1	0	1	1	1	0	0
$+2V_{dc}/3$	1	0	0	1	0	1	1	1	0	0
$+V_{dc}/3$	1	0	1	0	0	1	1	1	0	0
0	1	0	1	0	1	0	0	0	0	0
$-V_{dc}/3$	1	0	1	0	0	1	0	0	1	1
$-2V_{dc}/3$	1	0	0	1	0	1	0	0	1	1
$-V_{dc}$	0	1	0	1	0	1	0	0	1	1

Now the predicted future current values at $k+1$ instant for each switching states can be calculated from each voltage levels as:

$$i_{gn}(k+1) = i_{gn}(k)(1 - \frac{R_{fn}T_s}{L_{fn}}) + \frac{T_s}{L_{fn}}(v_{on}(k) - v_{gn}(k)) \quad (7)$$

Where $i_{gn}(k+1)$ and $i_{gn}(k)$ are the future and measured grid current values respectively, $v_{on}(k)$ and $v_{gn}(k)$ are the measured inverter output and grid voltages respectively. R_{fn} and L_{fn} being the grid filters, where n denotes the phases (a, b, c). Then the cost function which evaluates the error between reference current and predicted current values can be presented as:

$$g = (i_{refn}(k) - i_{gn}(k+1))^2 \quad (8)$$

This cost function will decide the best switching sequence which will be provided to the HMMC switches for switching.

3.3. Choosing Optimum Switching Sequence

After the cost function calculation for each voltage levels, the objective is to choose the optimum switching sequence. This is done by choosing the cost function with minimum value. It means, choosing the voltage level to generate the current, which will be the most closer to the reference current at $k+1$ instance. The whole process is summarized as flowchart in the Figure 4.

4. SIMULATION RESULTS

In this paper a 6kWatts three-phase system is simulated in the Matlab/Simulink environment. The real and reactive power references are provided manually for each phase. Various parameters taken for the simulation studies are given in Table 4. The system is studied for different values of real and reactive power demands by the grid.

The grid phase voltage is kept at 230 V olts RMS as shown in Figure 5(a). The changes in the real and reactive power references are done in different times as shown in Table 3.

Initially the HMMC has to give 3kWatts of real power to the grid until $t = 0.5$ Sec. The reactive power is maintained at 0 Vars, so the grid current has to be in phase with the grid voltage and the output power factor is maintained at unity. Then at $t = 0.5$ Sec the real power and reactive power reference is

increased to 6 kWatts and 3 kVars respectively. Figure 5(b), (c), and (d) shows the phase voltages and currents for phases (a, b, c). From the Figure 6, it can be seen that the response of the controller is quite fast enough to track the reference powers.

Table 3. Changes in real and reactive power references per phase

Time (Sec)	Real Power (Watts)	Reactive Power (Vars)
0	1000	0
0.5	2000	1000
0.55	2000	-1000
0.6	1000	1000

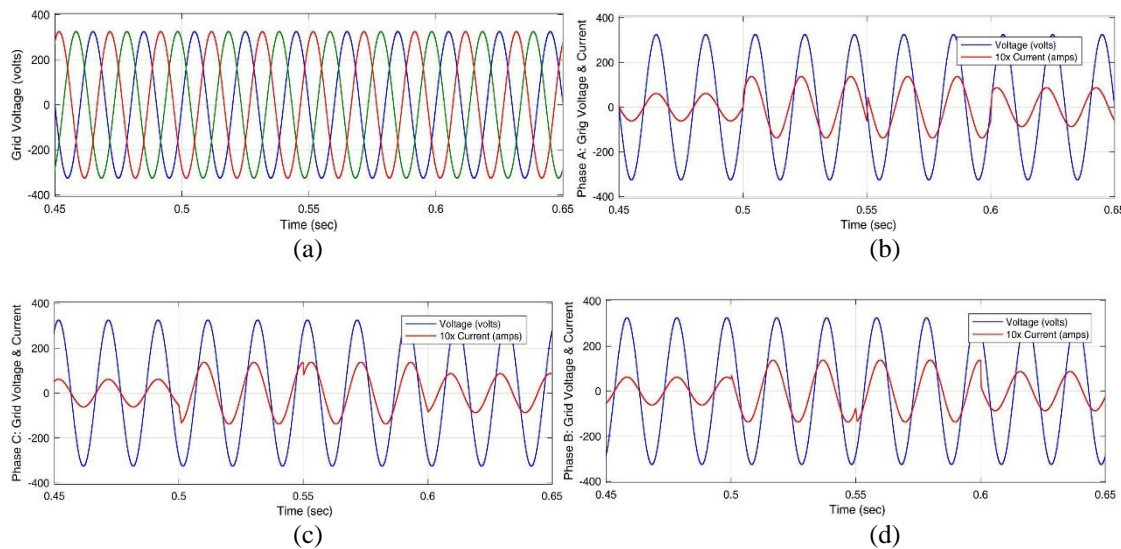


Figure 5. (a) Three-phase grid voltages, (b) Phase-a grid voltage and current, (c) Phase-b grid voltage and current, (d) Phase-c grid voltage and current.

The response of real and reactive power changes after changing the reference power demands can be seen in the Figure 7. The reference power are changed at times $t = 0.55$ Sec and 0.6 Sec.

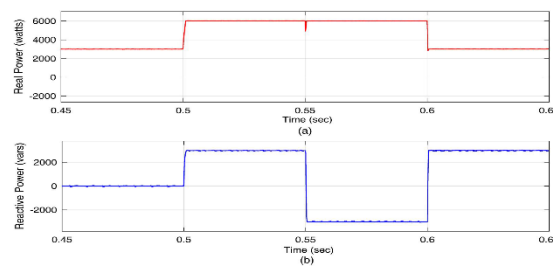


Figure 6. Changes in the real and reactive power demands by the grid.

During this time period the real power demand is kept at 6 kWatts and the reactive power is changed from 3 kVars to -3 kVars at time $t = 0.55$ Sec. With slight disturbances the real power is maintained constant even changing the reactive power demand at $t = 0.55$ Sec, which can be clearly seen in the Figure 6. Then at last the power references are kept at 3 kWatts and 3 kVars at time $t = 0.6$ Sec for real and reactive powers respectively. These results show the effectiveness and the response of the FCS-Predictive current control scheme. The HMMC provides the desired real and reactive power demanded by the grid without much delay.

Then the whole system is simulated for grid voltage swell and sag conditions. In this case keeping the reactive power demand at 0V ars, the real power demand is kept at 6kWatts. The grid voltage is increased by 20% of its RMS value as shown in Figure 7(a). The corresponding grid current is increased to match up the real power supply by the HMMC to the grid as shown in Figure 7(b). The real and reactive power is being plotted in Figure 7(c).

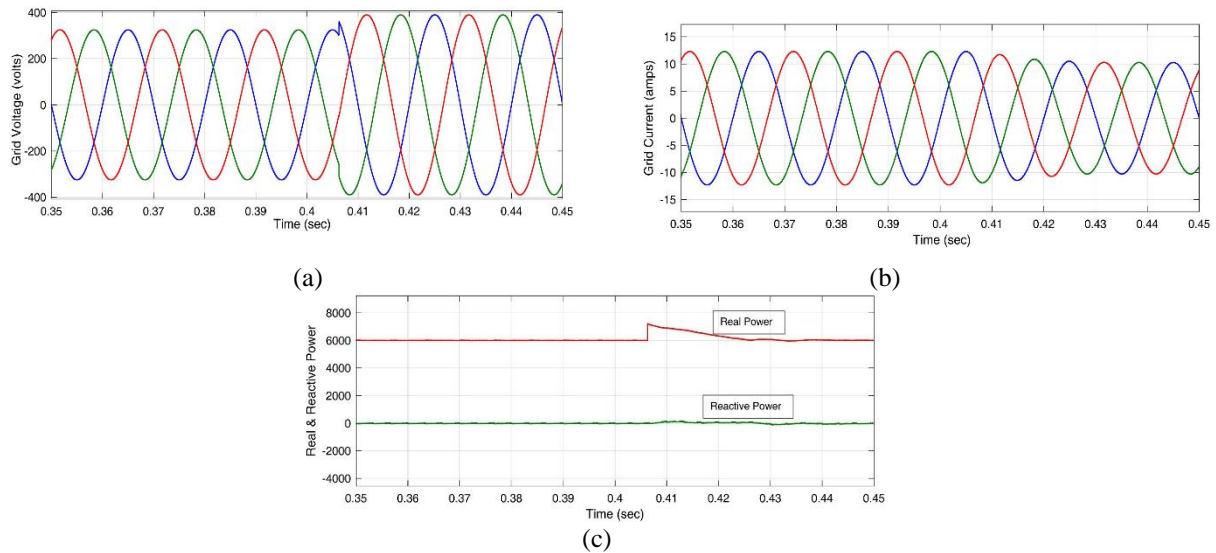


Figure 7. (a) Grid voltage, (b) Grid current, (c) Real and reactive power supply by HMMC to the grid, during swell condition

It can be observed from the Figure 8(c) that the voltage swell caused a slight increment in the real power as transient, but in very less time it came to reference value due to the fast response of the controller. Then the system is simulated for the sag condition in the grid voltage as shown in Figure 8(a). The grid voltage is decreased by 20% of its RMS value, and the corresponding grid current and the real and reactive power supply can be seen in Figure 8(b) and (c) respectively.

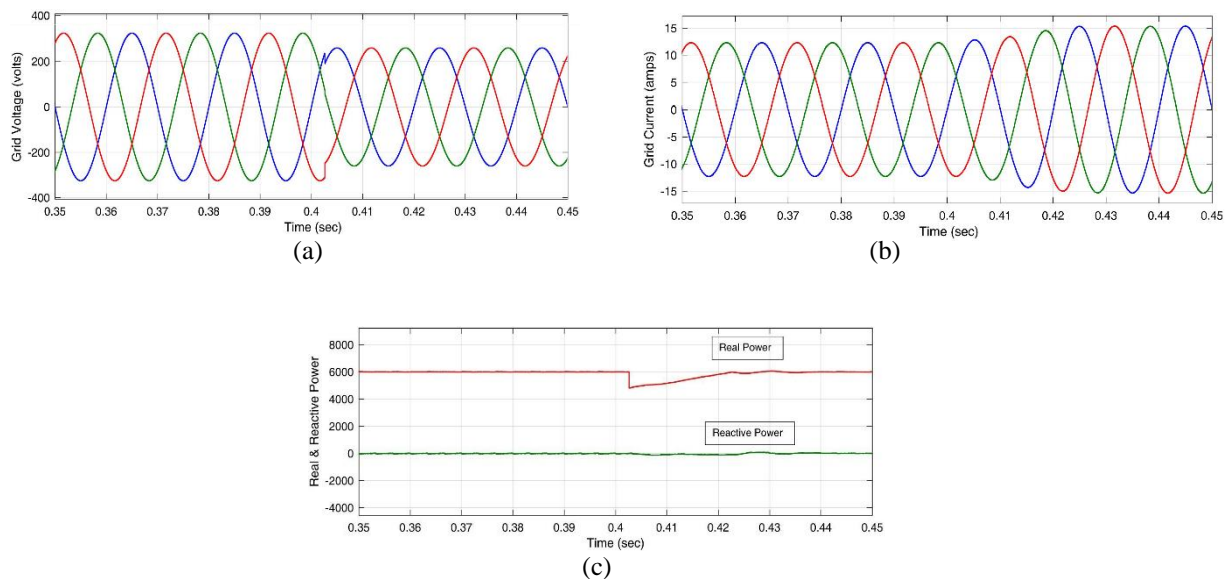


Figure 8. (a) Grid voltage, (b) Grid current, (c) Real and reactive power supply by HMMC to the grid, during sag condition.

5. CONCLUSION

This paper presents the grid application of a new topology named as Hybrid Modular Multilevel Converter (HMMC). This topology has reduced number of switch counts than the conventional MMC. Therefore it is more efficient and has less complexities in circuit design. A 6 kW *att* grid connected system is simulated for various real and reactive power demands. The Finite-Control-Set (FCS) Predictive Control scheme, which is growing its popularity in the power electronics applications is being employed here. This control scheme is quite easier in implementation than the conventional PI controllers because of the evolution of fast micro-controllers. From the simulation results it can be seen that the control action is very much effective and is having very fast response time to track the reference real and reactive powers.

Table 4. Various parameters taken for simulation study

Parameters	Symbols	Values
Fundamental Grid Frequency	f	50 Hz
Grid Phase Voltage	v_{gn}	230 V (RMS)
DC Input Filter	V_{dc}	400 V
Inductance Filter	L_{fn}	10 mH
Resistance	R_{fn}	0.01 Ω
Sampling Time	T_s	5 μ s
Simulation Time	t	1 s
Number of Sub-Modules Per-Phase	N	3
Sub-Module Capacitance	CSM	4700 μ F

REFERENCES

- [1] H. Abu-Rub, M. Malinowski, K. Al-Haddad, "Power Electronics for Renewable Energy Systems, Transportation and Industrial Applications," John Wiley & Sons, 2014.
- [2] J. Rodriguez, J. S. Lai, et al., "Multilevel Inverters: a survey of topologies, controls, and applications," *IEEE Trans. Ind. Electron.*, Vol. 49, No. 4, pp. 724-738, Aug. 2002.
- [3] R. Omar, M. Rasheed, et al., "Comparative Study of a Three Phase Cascaded H-Bridge Multilevel Inverter for Harmonic Reduction," *TELKOMNIKA Indonesian Journal of Electrical Engineering*, Vol.14, No. 3, pp. 481-492, 2015.
- [4] A. Lesnicar and R. Marquardt, "An innovative modular multilevel converter topology suitable for a wide power range," *Proc. of IEEE Power Tech.*, Bologna, Italy, June 2003.
- [5] *IEEE standard for interconnecting distributed resources with electric power systems*, IEEE Std 1547-2003, pp. 1-16, 2003.
- [6] *IEEE Guide for Monitoring, Information Exchange, and Control of Distributed Resources Interconnected with Electric Power Systems*, IEEE Std 1547.3, 2007.
- [7] M.A. Perez, S. Bernet, et al., "Circuit Topologies, Modeling, Control Schemes, and Applications Of Modular Multilevel Converters," *IEEE Trans. on Power Electron.*, Vol. 30, No. 1, Jan. 2015.
- [8] A. Dekka, B. Wu, R. L. Fuentes, et al., "Evolution of Topologies, Modeling, Control Schemes, and Applications of Modular Multilevel Converters," *IEEE Journal of Emerging Topics in Power Electron.*, Vol. PP, Issue: 99, Aug. 2017.
- [9] M. Hagiwara and H. Akagi, "Control and experiment of pulse width modulated modular multilevel converters," *IEEE Trans. on Power Electron.*, Vol. 24, No. 7, pp. 1737-1746, July 2009.
- [10] S. Rohner, S. Bernet, M. Hiller, and R. Sommer, "Modelling, Simulation and Analysis of a Modular Multilevel Converter for Medium Voltage Applications," in *Proc. IEEE Int. Conf. Ind. Technol.*, pp. 775-782, 2010.
- [11] B. S. Riar, T. Geyer and U. K. Madawala, "Model Predictive Direct Current Control of Modular Multilevel Converters: Modeling, Analysis, and Experimental Evaluation," *IEEE Trans. on Power Electron.*, Vol. 30, No. 1, Jan. 2015.
- [12] J. Scoltock, T. Geyer, and U. K. Madawala, "Model Predictive Direct Power Control for Grid-Connected NPC Converters," *IEEE Trans. on Industrial Electron.*, Vol. 62, No. 9, Sep. 2016.
- [13] A. Iqbal, et al., "Finite State Model Predictive Current and Common Mode Voltage Control for a Seven-phase VSI," *Int. Journal of Power Elect. and Drive Systems (IJPEDS)*, Vol. 6, No. 3, Jan. 2015. [14] A. Chatterjee, K. B. Mohanty, V. S. Kommukuri and K. Thakre, "Power quality enhancement of single phase grid tied inverters with model predictive current controller," *Journal of Renewable and Sustainable Energy*, Vol. 9, No. 1, Jan. 2017.
- [15] R. R. Behera and A. N. Thakur, "Hybrid Modular Multilevel Converter Based Single-Phase Grid Connected Photovoltaic System," *International Journal of Renewable Energy Research*, Vol. 7, No. 3, 2017.